THE INFLUENCE OF PARTICLE CONCENTRATION ON THE FLUID PHASE OF AN AXISYMMETRIC MULTIPHASE IMPINGING JET

J.E. Vickers, M. Fairweather and D. Harbottle

School of Chemical and Process Engineering, University of Leeds, Leeds LS2 9JT, UK

mn09jv@leeds.ac.uk

Abstract

Particle image velocimetry (PIV) is used to determine the effect of particle concentration on the fluid phase of a solid-liquid multiphase impinging jet. Two spherical particles were considered, polystyrene of 1050 kg m^{-3} and glass of 2450 kg m^{-3}, both with a diameter of 225 μm. The fluid axial and radial velocities are measured with particle volume fractions (φ) equal to 0, 1×10^{-4}, 2×10^{-4} and 4×10^{-4}. For both particle types as the concentration is increased, the level of axial velocity retained immediately prior to impingement (at 6 diameters from the pipe exit) also increases. At low particle concentrations the particles have little effect on the flow turbulence, however, at higher particle concentrations the particle effect becomes more significant, with a near doubling of the peak axial RMS velocity one diameter from the jet outlet in one case. The introduction of polystyrene particles has the effect of dampening radial and axial RMS velocities, except for at the highest concentration immediately after the jet outlet where the axial turbulence is enhanced by the particles.

1 Introduction

Multiphase particulate flows occur in a number of natural and industrial systems. As such, research into understanding the influence of these particles on the mechanics of the system is important in order to optimise plant equipment and maintain high safety standards.

The focus of this study is the effect of particle loading on the flow behaviour of an axisymmetric impinging water jet. Impinging jets are utilised for a variety of heat transfer, mass transfer, and mixing applications. However, this study was inspired by the impinging jets used to re-suspend nuclear waste in highly active storage tanks.

There is, however, a scarcity of data available for multiphase impinging jets. Tsuji et al. (1988) and Longmire and Eaton (1992) have undertaken relevant studies using a gas-solid system, with the former focusing on the effect of particle size, and particle loading being the focus of the latter. Yoshida et al. (1990) studied a gas-solid impinging jet, however, concentration effects were only examined with regards to heat transfer. Anderson and Longmire (1995) considered how variation in the particle Stokes number affected particle behaviour in an impinging jet using PIV. However, they assumed the influence on the gas carrier phase to be negligible. An earlier study by Modarress et al (1984) examined the role of particle concentration in a gas-solid free jet, finding that close to the jet outlet, as the concentration of the particle phase increased, the mean velocity remained unaffected. However, there was a definite decrease in the velocity fluctuations.

Other relevant work is due to Gore and Crowe (1989) who examined and plotted experimental data for a variety of multiphase jet and pipe systems, showing some correlation between the change in turbulence intensity due to particles and a length scale ratio made up of the particle diameter and a characteristic length of the most energetic eddies. This work was expanded upon by Hetsroni (1989) who proposed that small particles with low particle Reynolds numbers supress fluid turbulence, and particles with particle Reynolds numbers greater than 400 enhance it. Following on from this Elghobashi (1994) produced a map of regimes considering the effect of particle concentration, and the ratio of the particle response time to the Kolmogorov time scale, in order to attempt to predict the effect of particles on the carrier phase turbulence levels. This ratio, also known as the Stokes number, will henceforth be referred to as such.

2 Experimental method

The study was performed using a stainless steel pipe discharging vertically into a square based glass tank with the outlet positioned 6 pipe diameters from the impingement surface. The pipe was 600 mm in length to ensure fully developed turbulent flow, with an internal diameter of 4 mm and wall thickness of 1 mm, and was supported by a cross brace at the top of the tank. The supply of test fluid was via a centrifugal pump from a feed tank, and this contained an overhead stirrer to ensure the dispersion of the particles throughout the fluid. The feed line was connected to a needle valve allowing control and measurement of the flow rate. The valve was set to a flow rate of 0.045 L s^{-1} giving a flow Re at the nozzle exit of 14,795.

The selection of PIV was due to its less invasive nature and ability to capture the entire flow field at once. When compared with other measurement

techniques, such as hot wire anemometry, any disruption to the natural behavior of the flow is minimal as the equipment is external to the system. The PIV system, supplied by Dantec Dynamics (UK), utilised a Litron Nd:YAG laser to generate a <1 mm thick light sheet. This light sheet was timed to coincide with image capture by a Flowsense 2M camera equipped with a Sigma Macro Lens. Measurements were obtained via the cross correlation of 6,200 image pairs, with the images captured 50 µs apart.

The fluid velocities were measured using polymethyl methacrylate particles labelled with Rhodium B. The fluid axial and radial velocities were measured with particle volume fractions of 0, 1×10^{-4}, 2×10^{-4} and 4×10^{-4}. Two particle densities were investigated, with information for both the solids and tracer particles given in Table 1.

Table 1: Particle properties.

Particles	***Glass***	***Polystyrene***	***PMMA Tracers***
Diameter (µm)	225	225	10
Density (kg m^{-3})	2450	1050	1190
Response Time (ms)	6.9	2.9	0.0066
Settling Velocity (m s^{-1})	39.92 $\times10^{-3}$	1.37 $\times10^{-3}$	10.34 $\times10^{-6}$
Length Scale Ratio	0.563	0.563	0.025
Stokes Number	86	37	0.08

An Midopt orange-red long-pass filter (LP580) fitted to the camera screened out the larger particles, so only the smaller tracer particles were detected by the camera, therefore ensuring that the movement of the fluid was being tracked and not the dispersed phase. The introduction of fluorescent particles into the feed tank with the impinging jet loop running allowed a steady state homogenous dispersion to be reached. Measurement of the fluorescent tracer particles was then performed to obtain the baseline single-phase flow results in the absence of solid particles. The solid phase particles were then added at the relevant concentrations and the measurement repeated.

Cross correlation of the image pairs allowed the instantaneous velocities of the axial and radial components of the fluid to be resolved. The mean velocity was then calculated and from this a Reynolds decomposition gives the velocity fluctuations. By taking the root mean square of these fluctuations and dividing by the mean velocity the turbulence intensity is obtained.

3 Results and discussion

In order to compare the experimental flows, data profiles were taken at varying points across the jet, with an increase in X/D representing a greater distance from the impingement surface. All results are given relative to the maximum fluid axial velocity at the jet outlet (at 6 X/D). In the following figures, the results for the polystyrene particles are plotted against the left hand ordinate, and for the glass particles against a shifted right hand ordinate.

The jet outlet was positioned at 6 X/D and Figure 1 shows the first data profile for the mean axial velocity taken at 5 X/D (i.e. 1D from the outlet).

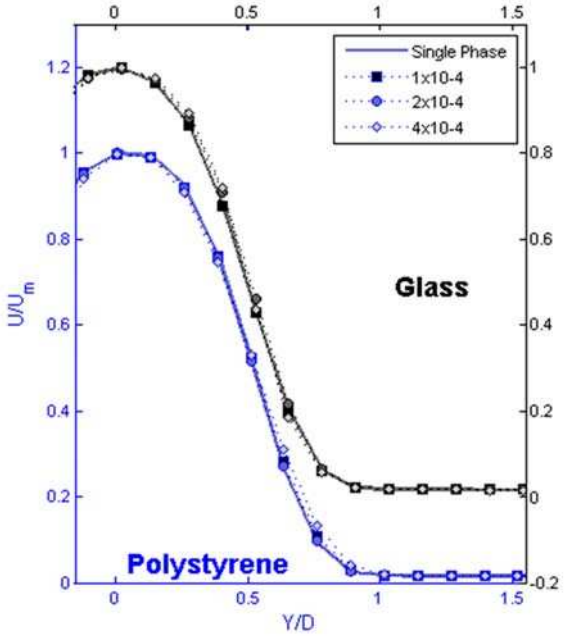

Figure 1: Axial mean velocity at 5 X/D.

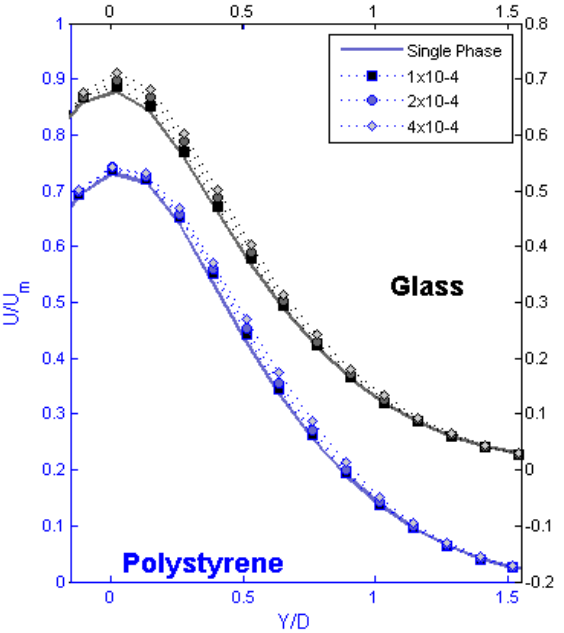

Figure 2: Axial mean velocity at 0.5 X/D.

At this flow position there is little change in the mean velocities as the particle concentration is increased. There is a very slight increase in the spreading rate of the jet as the concentration of less dense polystyrene particles is increased which is in contrast to what is observed for the glass particles

which at the same flow position have the opposite effect, i.e. the particles reduce the spreading rate of the jet, although to a lesser extent. This trend continues as the jet develops and progresses towards the impingement zone, with the effects of the impingement plate beginning around 0.5 X/D. At this point, the jet begins a rapid deceleration due to the pressure gradient exerted upstream by the impingement surface, as can be seen in Figures 2 and 3. For both the polystyrene and glass particles an increase in solids volume fraction corresponds with a greater retention of the mean velocity. This relationship is, however, not linear.

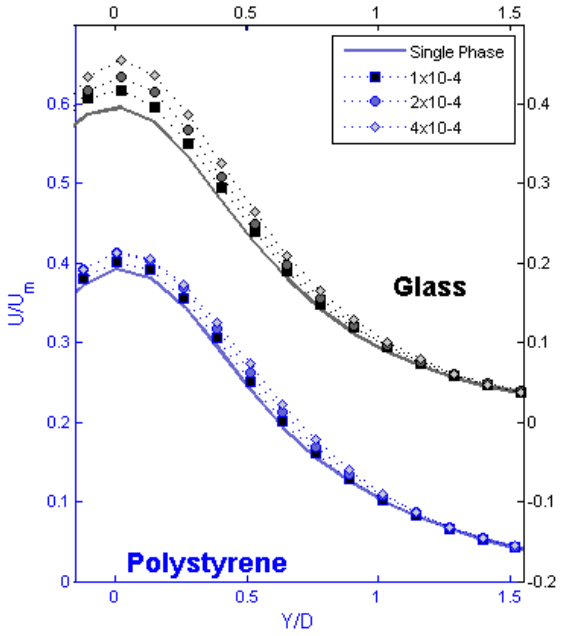

Figure 3: Axial mean velocity at 0.2 X/D.

As shown by Figure 3, when polystyrene particles are introduced at $\varphi = 1\times10^{-4}$ the axial mean velocity 0.2 X/D from impingement is 2% greater than for the single phase measurement, with this increasing to 5% at $\varphi = 2\times10^{-4}$ and maintaining this increase as φ rises further to 4×10^{-4}. The glass particles also reduced the deceleration of the jet with increased loading. When compared with the single phase measurements, $\varphi = 1\times10^{-4}$ gave a 6% increase, $\varphi = 2\times10^{-4}$ a 9% increase and $\varphi = 4\times10^{-4}$ a 15% increase in the axial mean velocity.

The glass particles, being significantly denser than the fluid, will resist the deceleration of the jet due to them having greater momentum than the surrounding fluid; this will cause energy to be transferred back to the fluid as the particles experience drag due to the velocity difference. This accounts for the effect of the glass particles. The polystyrene particles, however, are a similar density to the fluid and so this mechanism cannot explain the retention of velocity as the particle loading increases. A possible explanation for this is the reduction of turbulence caused by the addition of these particles that will discussed later.

The use of PIV allows radial velocity vectors to be obtained and resolved even in areas where the radial velocity is several orders of magnitude smaller than the axial velocity, e.g. at the location of the first profile after the nozzle exit, where the peak radial mean velocity is around 2% of the maximum axial value (Figures 1 and 4). This peak velocity is towards the jet centreline showing that in this region the dominant radial property is the entrainment of the surrounding fluid, which accelerates towards the jet until it reaches the turbulent mixing layer.

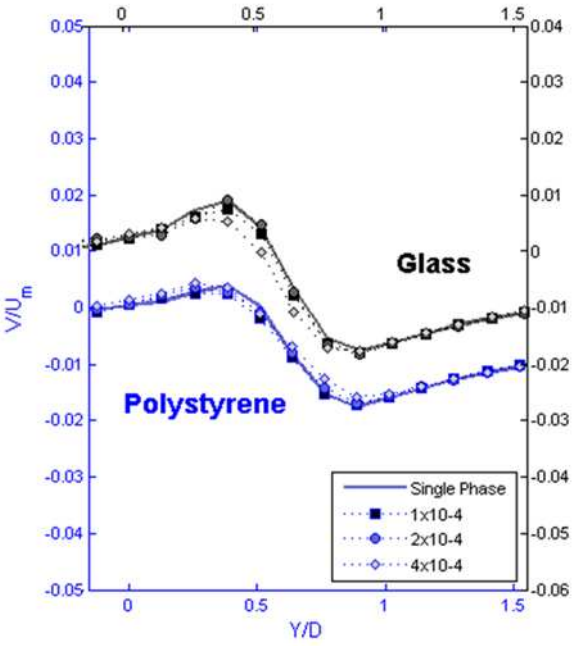

Figure 4: Radial mean velocity at 5 X/D.

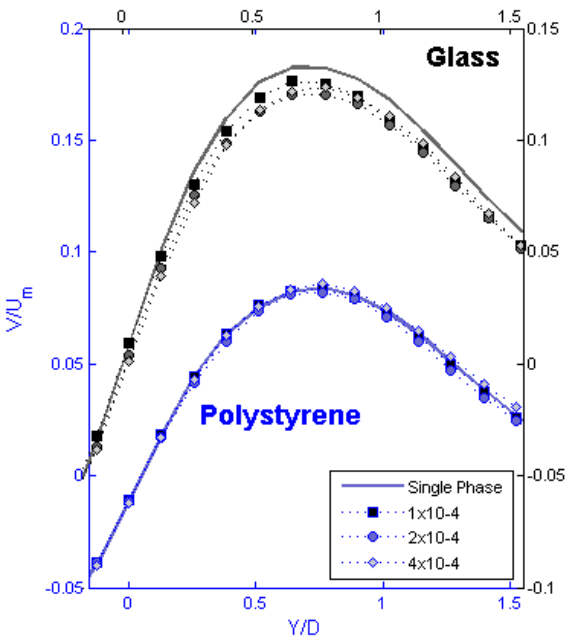

Figure 5: Radial mean velocity at 0.5 X/D.

At this point, in the mixing layer, the radial mean

velocity rapidly approaches zero, maintaining this throughout the potential core of the jet release. As the jet develops downstream the region with no radial velocity shrinks and the shear mixing layer expands, causing the radial velocity away from the centreline to increase within the jet. With further development, there is a reduction in the maximum radial mean velocity of the entrained surrounding fluid and the flow away from the centreline becomes dominant. Figure 5 shows that the rapid deceleration axially of the jet as it approaches the impingement zone coincides with a radial acceleration of the jet, this being first apparent at 0.5 X/D where the peak radial velocity has increased from 2% of the maximum outlet velocity to 10%.

This continues as the jet reaches the impingement surface, with the magnitude of the peak radial mean velocity surpassing that of the peak axial velocity between 0 and 0.2 diameters from the impingement surface. For the closest measurements taken to the base of the tank, the radial velocity peaks at 33% of the maximum axial velocity, as seen in Figure 6.

Concerning the influence of particles on the mean radial velocities there is very little effect. The glass particles appear to slightly reduce the radial velocity within the jet and maintain this effect from the nozzle to impingement, with the effect becoming more pronounced as the jet develops and with an increase in concentration amplifying the effect. The polystyrene particles do not show this damping until the profiles at 0.2 X/D. Similarly to the axial measurements, the two highest concentrations ($\varphi = 2\times10^{-4}$ and $\varphi = 4\times10^{-4}$) of polystyrene particles have very little difference between them.

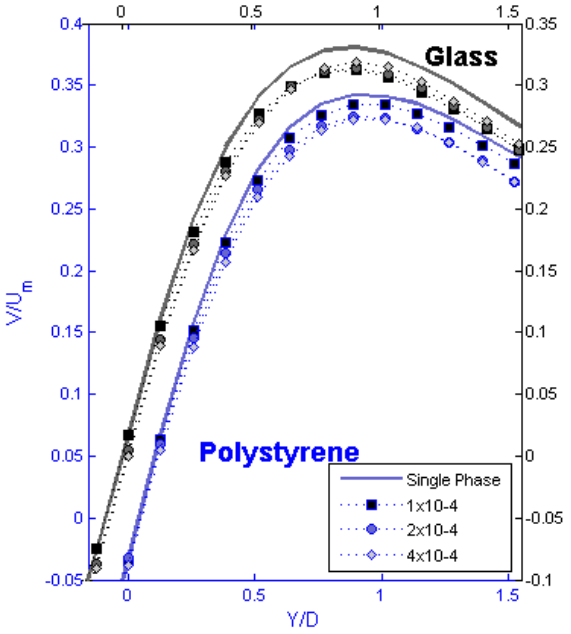

Figure 6: Radial mean velocity at 0.2 X/D.

The axial turbulence measurements displayed in Figures 7-9 clearly show the expected twin peaks caused by the increased turbulence within the turbulent mixing layer surrounding the potential core. This region within the jet is where turbulence is greatest, with momentum transfer from the jet to the ambient fluid as entrainment occurs and the jet grows.

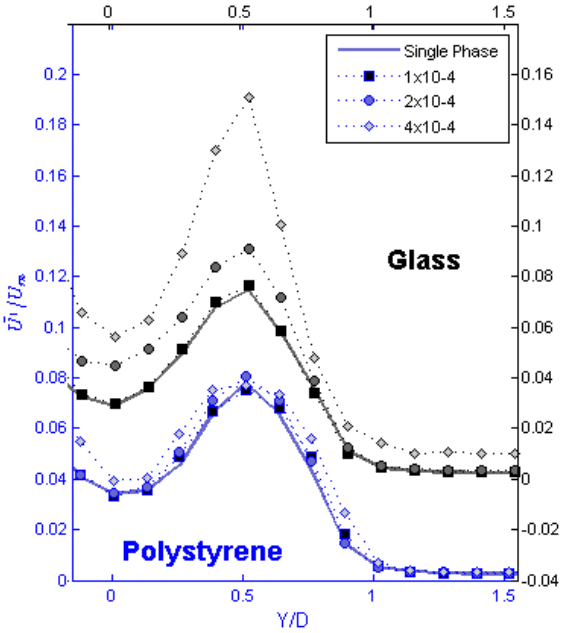

Figure 7: Axial RMS velocity at 5 X/D.

At 5 X/D the introduction of glass particles causes an increase in the axial turbulence intensity. At the lowest concentration this increase is minimal, ~ 5%, however at the highest concentration the peak turbulence levels are almost double the single phase values. At the same location the polystyrene particles have very little effect, with the highest concentration tested causing a maximum 6% increase in the axial turbulence intensity. As the jet develops this is no longer the case.

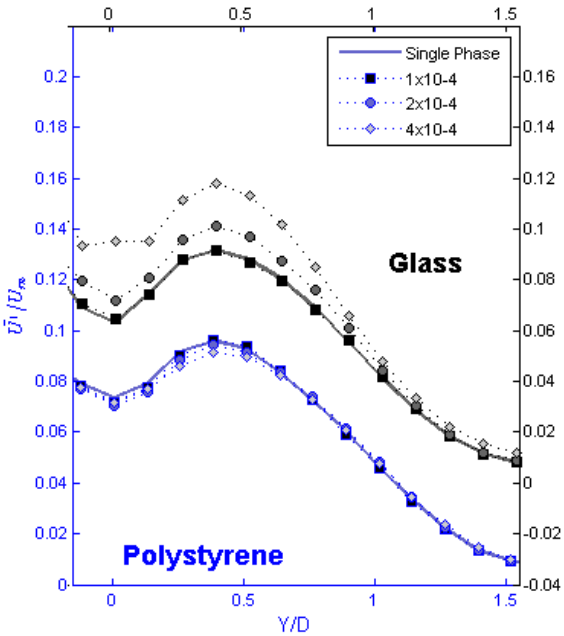

Figure 8: Axial RMS velocity at 1 X/D.

Figure 8 shows that at one diameter from impingement the lowest concentration of glass particles is almost indistinguishable from the single phase flow, and the difference between the single phase and the highest particle concentration ($\varphi = 4\times10^{-4}$) has reduced to 1.29 times that of the single phase. This reduction is caused by both an increase in the turbulence intensity of the single phase as the jet develops and a reduction in the peak turbulence intensity of the most heavily laden flow. The polystyrene particles at this point are no longer enhancing the turbulence but diminishing it, with an increase in the solids concentration having a greater effect, although the magnitude of this effect is much smaller than the enhancement caused by a similar loading of glass particles.

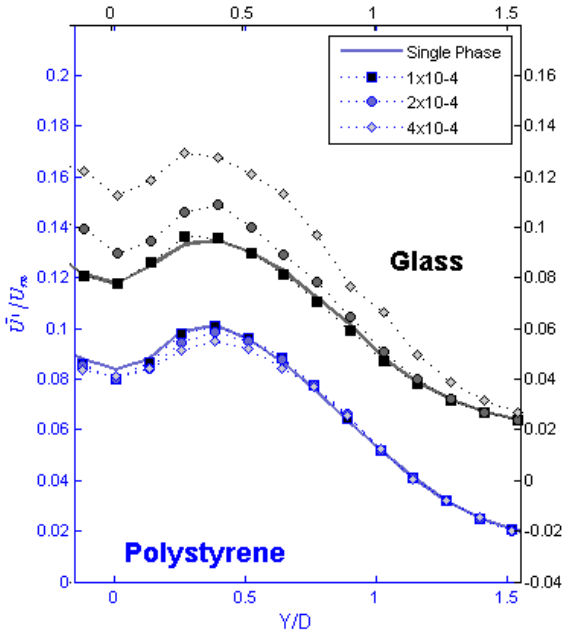

Figure 9: Axial RMS velocity at 0.5 X/D.

At a volume fraction of 4×10^{-4} there is a reduction in the peak axial turbulence of 6%. This effect is also seen in the 0.5 X/D profiles, with peak and centreline axial turbulence reduced. As mentioned previously, this is a possible mechanism for the retention of fluid velocity as less energy is lost to viscous dissipation. The glass particles continue to enhance the turbulence as the impingement zone is reached, as can be seen in Figure 9.

Similarly to the axial turbulence measurements, the introduction of very low particle concentrations (i.e. $\varphi = 1\times10^{-4}$) of both the glass and polystyrene particles has very little effect on the intensity of the radial turbulence. At the 5 X/D location, shown by Figure 10, increased loading of the glass particles causes an increase in the radial turbulence whereas an increased volume fraction of the polystyrene particles works to reduce the magnitude of the radial turbulence fluctuations. This effect is maintained throughout the jet development region before the pressure gradient created by the impingement surface is encountered.

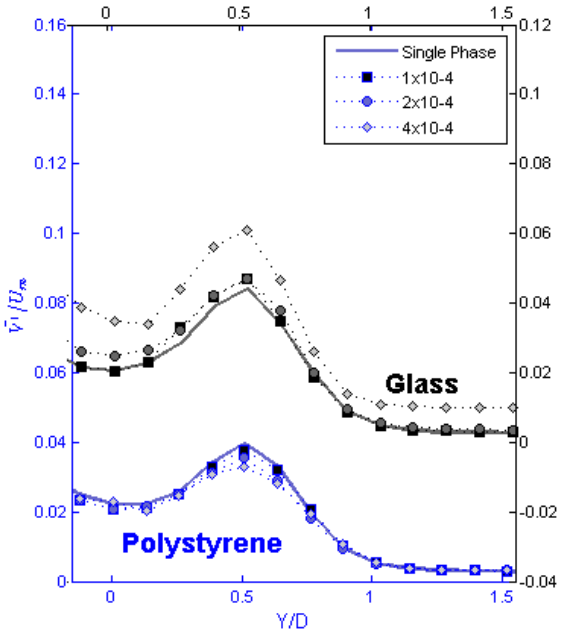

Figure 10: Radial RMS velocity at 5 X/D.

As the jet progresses downstream radial turbulence increases at all particle concentrations and for both particle types in this jet development region, although the highest concentration of glass particles does not give the same magnitude of increase when compared with the single phase measurements. Between 5 X/D and 1X/D (Figures 10 and 11) the single phase flow experiences a 26% increase in peak radial turbulence fluctuations compared with only 14% when $\varphi = 4\times10^{-4}$.

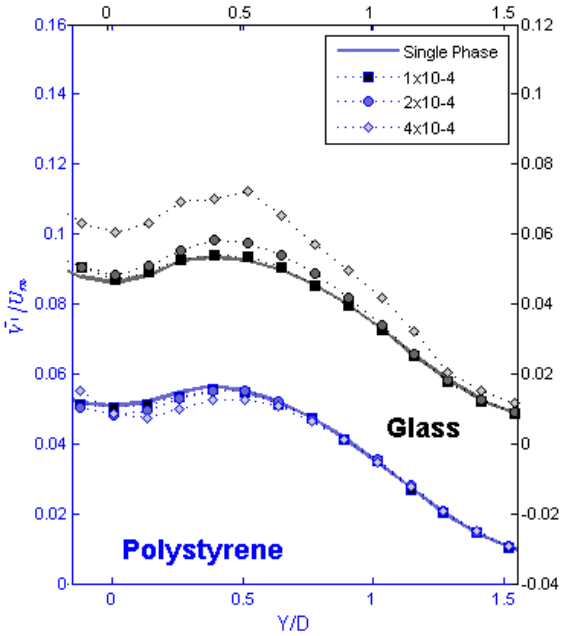

Figure 11: Radial RMS velocity at 1 X/D.

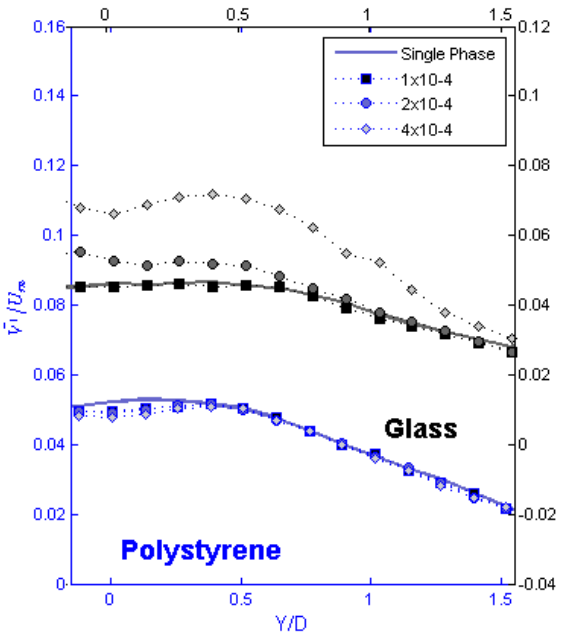

Figure 12: Radial RMS velocity at 0.5 X/D.

As the jet approaches the impingement surface the distinctive peaks of the mixing layer are diminished and finally lost, except in the presence of higher concentrations of glass particles where the distinctive shape is retained, suggesting that the glass particles cause an extension of the mixing layer of the jet. This can be seen in Figure 12. This is significant as many heat transfer applications rely on the use of such jets to maximise thermal transfer. In the immediate region before impingement, the polystyrene particles reduce the radial turbulence fluctuations at solid loadings of 1×10^{-4} and 2×10^{-4}, but at 4×10^{-4} the addition of particles results in a slight increase when compared with the single phase measurements.

4 Conclusions

As shown by authors such as Tsuji et al. (1988) and Yoshida et al. (1990), there is a reduction in the spreading rate of the jet with the introduction of particles, as well as a reduction in the velocity decay rate. The effect is more pronounced in the impingement region, with the particles causing the fluid to retain more velocity.

The effect of the particles on modulating the turbulence field was dependant on particle concentration, density and the region of the jet being examined. The less dense polystyrene particles enhance turbulence immediately after the nozzle, however, as the jet develops, this changes and the presence of the particles causes a reduction in the turbulent fluctuations. In contrast, the glass particles enhance turbulence at all measurement locations, although this effect is minimal at low concentrations.

As the two particles examined are of equivalent diameter, the measured fluid effects cannot be simply described by the approach presented by Gore and Crowe (1989). Their work does suggest, however, that as a jet develops there is the potential for a particle to change from enhancing turbulence to dissipating it as the size of the turbulent eddies increases. In the current work, using the formula they applied to predict the characteristic length of the most turbulent eddies, the ratio of particle diameter to characteristic length does not drop below the suggested threshold of 0.1 at which the transition from enhancement to dissipation is predicted to occur.

Particle velocities were not measured in this study so the relationship suggested by Hetsroni (1989) could not be investigated (although such measurements are ongoing). The more complicated relationship between the particles and their effects suggested by Elghobashi (1994) also has problems when applied to both particle densities as if the characteristic length is calculated so as to account for the dissipation effect of the polystyrene particles, then it also suggests that the glass particles should also cause dissipation of turbulence. Further work on a range of particle sizes and densities is needed to further explore this.

Acknowledgement

The work reported was supported by Sellafield Ltd. and the University of Leeds through their Nuclear Fuel Cycle CDT.

References

Anderson, S.L. and Longmire, E.K. (1995), Particle motion in the stagnation zone of an impinging air jet, *J. Fluid Mech.*, Vol. 299, pp. 333-366.

Elghobashi, S. (1994), On predicting particle-laden turbulent flows, *Appl. Sci. Res.,* Vol. 52, pp. 309-329.

Gore, R. and Crowe, C.T. (1989), Effect of particle size on modulating turbulent intensity, *Int. J. Multiphase Flow*, Vol. 15, pp. 279-285.

Hetsroni, G. (1989), Particles-turbulence interaction, *Int. J. Multiphase Flow*, Vol. 15, pp. 735-746.

Longmire, E. and Eaton, J. (1992), Structure of a particle-laden round jet, *J. Fluid Mech.*, Vol. 236, pp. 217-257.

Modarress, D., Wuerer, J. and Elghobashi, S. (1984), An experimental study of a turbulent round two-phase jet, *Chem. Eng. Commun.*, Vol. 28, pp. 341-354.

Tsuji, Y., Morikawa, Y., Tanaka, T., Karimine, K. and Nishida, S. (1988), Measurement of an axisymmetric jet laden with coarse particles, *Int. J. Multiphase Flow*, Vol. 14, pp. 565-574.

Yoshida, H., Suenaga, K. and Echigo, R. (1990), Turbulence structure and heat transfer of a two-dimensional impinging jet with gas-solid suspensions, *Int. J. Heat Mass Tran.,* Vol. 33, pp. 859-867.